The Membrane Lateral Pressure-Perturbing Capacity of Parabens and Their Effects on the Mechanosensitive Channel Directly Correlate with Hydrophobicity[†]

Kishore Kamaraju and Sergei Sukharev*

Department of Biology, University of Maryland, College Park, Maryland 20742

Received June 10, 2008; Revised Manuscript Received August 4, 2008

ABSTRACT: Lipid bilayers provide a natural anisotropic environment for membrane proteins and can serve as apolar reservoirs for lipid-derived second messengers or lipophilic drugs. Partitioning of lipophilic agents changes the lateral pressure distribution in the bilayer, affecting integral proteins. *p*-Hydroxybenzoic acid esters (parabens) are amphipathic compounds widely used as food and cosmetics preservatives, but the mechanisms of their broad antibacterial action are unknown. Here we describe effects of ethyl, propyl, and butyl parabens on the gating of the bacterial mechanosensitive channel of small conductance (MscS) and compare them with the surface activity and lateral pressure changes measured in lipid monolayers in the presence of these substances. Near the bilayer−monolayer equivalence pressure of 35 mN/m, ethyl, propyl, or butyl paraben present in the subphase at 1 mM increased the surface pressure of the monolayer by 5, 12.5, or 20%, respectively. No spontaneous activation of MscS channels was observed in patch−clamp experiments with parabens added from either the cytoplasmic or periplasmic side. Increasing concentrations of parabens on the cytoplasmic side of excised patches shifted activation curves of MscS toward higher tensions. A good correlation between the pressure increases in monolayers and shifts in activation midpoints in patch−clamp experiments suggested that the more hydrophobic parabens partition more strongly into the lipid and exert larger effects on channel gating through changes in lateral pressure. We show that cytoplasmically presented ethyl or butyl parabens both hasten the process of desensitization of MscS and influence inactivation differently. The higher rate of desensitization is likely due to increased lateral pressure in the cytoplasmic leaflet surrounding the gate. Neither of the parabens strongly affects the rate of recovery and does not seem to penetrate the TM2−TM3 interhelical clefts in MscS. We conclude that the bacterial mechanosensitive channel MscS provides a sensitive readout of lateral membrane pressure exerted by amphipathic molecules but may not be the primary target for the parabens in their antimicrobial activity.

The lipid component of cellular membranes provides a special environment for integral proteins, which is characterized by a high degree of anisotropy and asymmetry due to the orientation and differential distribution of phospholipids in the two membrane leaflets. Bearing a variety of headgroups and acyl chains, phospholipids and other components differently interact with membrane proteins and are shown to exert their effects on the folding and function of enzymes (*1, 2*), receptors (*3*), channels (*4*−*7*), and transporters (*8*−*10*). Oriented lipids are typically organized in a two-dimensional liquid-crystalline sheet stabilized by a network of lateral polar interactions between the headgroups. In the transversal direction, the boundaries between the polar and apolar regions generate a complex pressure profile across the fully hydrated bilayer (*11*−*14*). This pressure−tension distribution arising from multiple types of interactions may substantially depend on the bilayer composition. For example, due to the smaller size of the phosphatidylethanolamine (PE)[1] headgroup, bilayers made of PE are expected to have stronger pressure in the region of hydrophobic tails and weaker pressure in the polar region than those in phosphatidylcholine (PC) bilayers (*15*).

Lipophilic or amphipathic compounds that penetrate into the membrane can modify the chemical composition of certain layers at the same time, distorting the lateral pressure profile. General anesthetics (such as halogenated ethers) generally obeying the Meyer−Overtone rule massively partition into the hydrophobic core or boundary layers of the lipid bilayer, and their activating or inhibitory (*16*−*19*) effects on membrane channels and receptors have been ascribed to the changes in the lateral pressure distribution (*12, 20*).[1] Local anesthetics, typically charged amphipathic molecules, also contribute to the lateral pressure which was demonstrated in experiments with lipid monolayers (*21*). Besides surface activity, the molecular size and the area perturbation of the membrane caused by transient incorporation of the drug

[†] The work was supported by NIH Grant R01GM075225 to S.S.

* To whom correspondence should be addressed: Department of Biology, Bldg. 144, University of Maryland, College Park, MD 20742. E-mail: sukharev@umd.edu. Phone: (301) 405-6923. Fax: (301) 314-9358.

[1] Abbreviations: MscS, mechanosensitive channel of small conductance; MscL, mechanosensitive channel of large conductance; parabens, *n*-acyl esters of *p*-hydroxybenzoic acid; PE, phosphatidylethanolamine; PC, phosphatidylserine; TPE, total polar lipid extract from *Escherichia coli*; HEPES, 4-(2-hydroxyethyl)-1-piperazineethanesulfonic acid; HSPC, high-speed pressure clamp apparatus.

10.1021/bi801092g CCC: $40.75
Published on Web 09/17/2008

define its penetrating capacity (*22*). Asymmetric area stress in membranes caused by intercalation of amphipathic substances has also been analyzed (*23, 24*).

Mechanosensitive ion channels that directly respond to tension in the lipid bilayer are especially susceptible to distortions of the lateral pressure profile. Early works by Martinac and co-workers demonstrated that hydrophobic ions (trinitrophenol) and local anesthetics (chlorpromazine) increase the activity of a bacterial mechanosensitive channel of small conductance which was explained as an effect of tension redistribution between the leaflets (*25*). Lysolipids characterized with a stronger partitioning into membranes than anesthetics were found to be potent activators of the bacterial mechanosensitive channel of large conductance MscL when added asymmetrically on one side of the membrane (*26*). Reconstitution of MscL into PE liposomes increased its activating tension compared to the PC environment, which corroborates well the increased pressure acting on the centrally positioned gate of this channel (*27*). Mammalian potassium channel TREK was shown to be modulated by a variety of lipophilic agents such as lysolipids, fatty acids, diacyl glycerols, and local anesthetics (*28, 29*).

The motivation for the experiments described here came from the simple notion that esters of *p*-hydroxybenzoic acid (parabens) widely used as food and cosmetics preservatives for the past four decades (*30*) are in fact substances with a pronounced amphipathicity. With the increased length of the alkyl chain (methyl through butyl), the solubility of parabens in aqueous phase drops (*31*−*33*), whereas the extent of partitioning into *n*-hexane and *n*-octanol increases, which parallels the increased antibacterial potency (*34*). Previously published data demonstrated that parabens have a cytostatic effect on bacteria very similar to that of local anesthetics (*35*). More hydrophobic parabens require lower concentrations for the antimicrobial action, and early studies suggested that transmembrane proteins and transport systems may be the primary targets for long chain parabens (*34, 36, 37*).

Decades of use as food and cosmetics preservatives proved that parabens are generally safe for human health (*30*), although a small effect of transactivation of the estrogen receptor has been detected (*38*). This warranted studies on mammalian cells which have shown that parabens can inhibit normal release of lysosomal enzymes from lymphocytes (*39*), inhibit mitochondrial respiration in hepatocytes (*40*), and cause reversible modulation of voltage- and ligand-gated channels (*41*), again with butyl paraben being the most potent. More recent studies revealed activation of a pain receptor channel (TRPA1) by methyl paraben (*42*), and the mechanosensitive TRPY1 in yeast vacuole can also be directly activated by propyl paraben (*43*). Although many authors agree that the propensity of long chain parabens for membranes likely defines their cytostatic action along with some side effects, the mechanism of their broad antimicrobial potency remains unknown, and even the water−membrane partitioning of parabens has not been studied in sufficient detail.

In this paper, we characterize the membrane-perturbing effects of ethyl, propyl, and butyl parabens by measuring their surface activity and changes in the surface pressure in lipid monolayers. We apply these substances to native membrane patches containing bacterial mechanosensitive channel MscS and observe shifts in activating tension which parallel the pressure changes observed in monolayer experiments. We also describe substantial changes in the rates of MscS desensitization and inactivation by parabens and discuss the observations in the framework of the asymmetric location of the gate and modified lateral pressure profile in the bilayer.

MATERIALS AND METHODS

Surface Tension Measurements and Monolayer Experiments. Ethyl, propyl, and butyl esters of *p*-hydroxybenzoic acid (parabens) were purchased from Sigma-Aldrich (St. Louis, MO). Surface tensions of subphase solutions containing different concentrations of parabens were determined using the standard Wilhelmy method with a strip of filter paper (Whatman, No. 1, 10.5 mm wide and 0.25 mm thick) used as a plate. The pressure sensor (model 601, NIMA, Coventry, U.K.) was precalibrated using a 100 mg weight, after which the surface tension of pure water was determined to be −72 mN/m. At this stage, the pressure sensor was set to zero and subsequent measurements of surface tension produced positive values of surface pressure.

A rectangular Teflon monolayer trough (total area of ∼550 cm^2) with a single movable barrier (NIMA) enclosed in an air-clean bench was used in all experiments. The surface pressures were measured with the same Wilhelmy method. *Escherichia coli* total polar lipid extract (TPE) in chloroform was purchased from Avanti Polar Lipids (Alabaster, AL). The procedure of lipid preparation included removal of chloroform under the stream of nitrogen in a preweighted glass vial followed by drying under vacuum for 1 h. The vial was then carefully weighed, and lipids were dissolved by being vortexed in pure chloroform to a final concentration of 2 mM (1.53 mg/mL for TPE). Spreading of lipids on the aqueous subphase was done using a gastight 50 μL Hamilton syringe. The subphase buffer consisted of 100 mM KCl and 5 mM KH_2PO_4 and was titrated with KOH to pH 7.4. Due to limited solubility, parabens were added into the prewarmed (to ∼50 °C) subphase buffer to a desired concentration and thoroughly mixed on a stirring plate. Parabens stably remained in solution after cooling to room temperature. Compression (pressure−area) isotherms were measured at room temperature (22 °C) at a speed of 20 cm^2/min.

Electrophysiology. Giant *E. coli* spheroplasts were prepared with the standard technique (*44*) utilizing cephalexin as a septation blocker. The MJF 465 (*mscS*$^-$/*mscK*$^-$/*mscL*$^-$) (*45*) strain was used to express wild-type (WT) MscS. Patch−clamp recordings of MscS were performed exactly as described by Akitake et al. (*46*). Electrodes were pulled from borosilicate capillaries to a bubble number of 4.5 (resistance of 2.8 ± 0.2 MΩ, in a buffer with a specific conductivity of 39 mS/cm). Recordings were performed in symmetrical potassium [200 mM KCl, 45 mM $MgCl_2$, 5 mM $CaCl_2$, and 5 mM HEPES titrated to pH 7.4 with KOH] buffers in the pipet and bath. The bath solution was the pipet solution with a 400 mM sucrose supplement to osmotically stabilize spheroplasts. Parabens were delivered into the bath through a laboratory-built perfusion system, and the MscS activation midpoints were determined with 1 s ramp stimuli within 3 min of perfusion. The measurements of desensitization and inactivation were typically carried out 10 min after perfusion to allow for deeper equilibration. To apply parabens

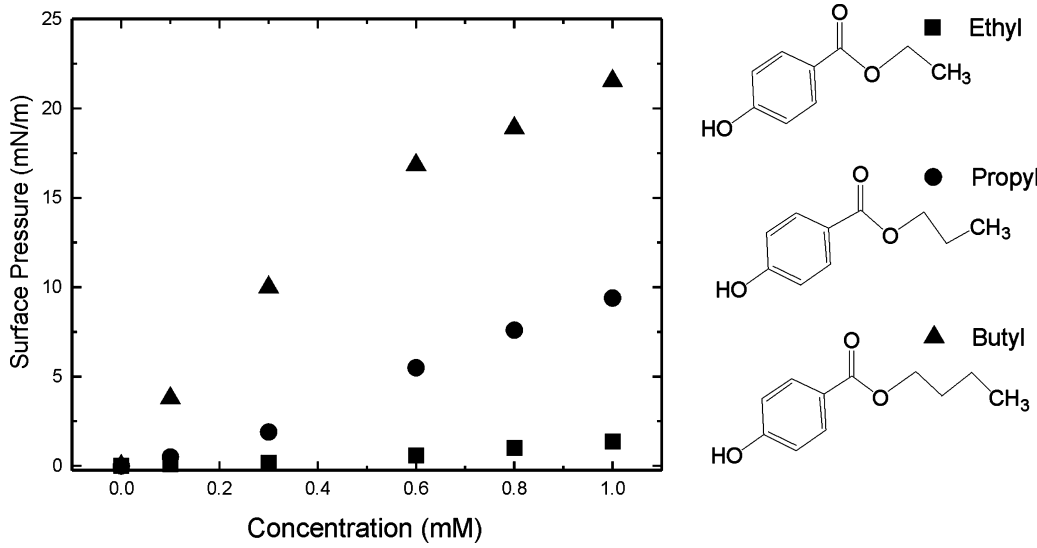

FIGURE 1: Surface activity of ethyl, propyl, and butyl parabens measured in the "subphase" buffer using the standard Wilhelmy method. The surface pressure corresponds to the reduction of the surface tension of the solution compared to that of the pure buffer. Ethyl paraben is the least and butyl paraben the most hydrophobic.

to the patch from the extracellular side, the tip of the pipet (~1 mm) was first filled with paraben-free buffer supplemented with 0.4 M sucrose and then the pipet was backfilled with the paraben-containing buffer. Slow diffusion of paraben to the tip and incorporation onto the outer leaflet were observed as changes in the activation midpoints for MscS over 30 min. Pressure ramps were applied using an HSPC-1 (ALA Scientific Instruments) high-speed pressure clamp apparatus controlled via the analog output from the DigiData1320A instrument. An ALA P-V unit upgraded with a stronger suction pump was used as the pressure and vacuum source. Vacuum and pressure were calibrated at both the pumps and the headstage using a PM015D pressure monitor (World Precision Instruments). Pressure traces were then recorded directly from the HSPC-1 headstage. Output commands to the HSPC-1 apparatus were controlled by Axon pClamp9 software in episodic stimulation mode (Axon Instruments).

RESULTS

Surface Activity of Parabens and Their Propensity for Lipid Monolayers. As preservatives in different formulations, parabens have sufficient antimicrobial effects at concentrations between 10^{-5} and 10^{-3} M (*34*). We measured surface tensions of the aqueous buffer used for subsequent monolayer experiments, in this range of concentrations. As shown in Figure 1, ethyl paraben is the least surface active and most hydrophilic among the three parabens while butyl paraben is the most hydrophobic and has the highest propensity for the air−water interface. When present in the solution at a concentration of 1 mM, ethyl paraben decreased the surface tension of an aqueous solution by 1.4 mN/m, propyl paraben by 9.4 mN/m, and butyl paraben by 21.5 mN/m. The surface tension of the aqueous solution with the salts and buffer was 71 mN/m. The surface activity of the three parabens agrees well with the published data for aqueous solubility (*31, 32*) and their partitioning in *n*-hydrocarbon/water and aliphatic alcohol/water systems (*47*).

E. coli polar lipid extract which is similar in composition to the inner membranes of the bacterium was chosen for formation of lipid films. The monolayer experiments were conceived to correlate surface pressure changes in the presence of parabens with their effects on activating tension of MscS residing in the inner membrane of *E. coli*. Compression ($\pi-A$) isotherms were recorded with paraben concentrations in the subphase ranging from 0 to 1 mM. The isotherms presented in Figure 2 are scaled against the surface pressure of pure buffer without lipid or paraben, taken to be zero. As seen from the plots, the surface pressure of monolayers in their most expanded state (right end of the curves) varies with the paraben concentration. The strongest upshift is observed for butyl paraben and reflects primarily its own partitioning into the air−water interface since the contribution to surface pressure due to the lipid molecules present in low density (two-dimensional gaseous phase) is negligible. Without lipids, the surface pressure of the pure paraben monolayer does not change with the position of the barrier as area changes do not affect the surface bulk equilibria for these substances. With lipids at the surface, compression of the monolayer in the presence of parabens in the subphase produces isotherms that lie above the control isotherm, indicating extra pressure created by the paraben intercalated between the lipids. For ethyl and propyl parabens, the difference between the control isotherm and the actual isotherm progressively increases with paraben concentration toward the middle of isotherms (area of ~120 Å^2/molecule) that reflects the excess chemical potential of favorable paraben−lipid mixing that stabilizes parabens at the interface between the lipids. At a high degree of compression, near the point of collapse (top left corner), isotherms taken at different concentrations essentially converge, indicating that the increasing lateral pressure gradually "squeezes" parabens out of the film into the bulk. The retention in the monolayer clearly correlates with the hydrophobicity of the paraben.

The collapse pressure of the monolayer for all parabens was around 45 mN/m and remained unchanged, indicating that up to a concentration of 1 mM these substances do not promote collapse of the lipid film. The average area per molecule for the lipid with no paraben in the subphase at 45

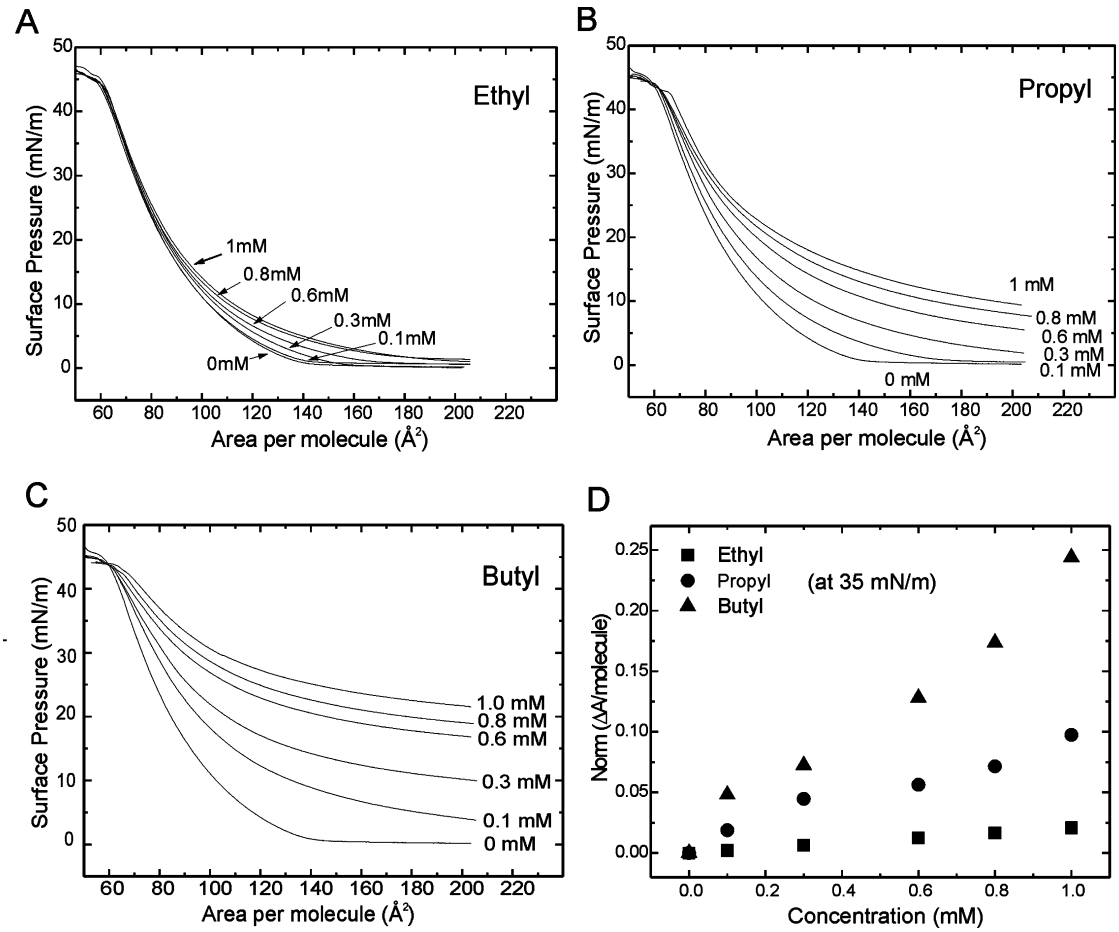

FIGURE 2: Pressure−area (π−A) isotherms of monolayers prepared from total polar *E. coli* lipids with ethyl paraben (A), propyl paraben (B), and butyl paraben (C) in the subphase. (D) Relative molecular area increase (ΔA per molecule) as a function of paraben concentration. The calculated ΔA per molecule was normalized to A per molecule at 35 mN/m in the absence of paraben. Isotherms were recorded at room temperature.

mN/m was ~60 Å^2, consistent with previously published data (*48, 49*). The increase in paraben concentration shifts the isotherms upward and to the right, effectively increasing pressure in the entire range of molecular areas. The shifts of the isotherms are subtle in the presence of ethyl paraben and more pronounced in the presence of butyl paraben. At the monolayer−bilayer equivalence pressure of 35 mN/m and paraben concentration of 1 mM in the subphase, the increase in the area per molecule of the lipid was 2.5% for ethyl, 10% for propyl, and 25% for butyl paraben. At this pressure, *E. coli* polar lipids on average occupy 68.5 Å^2/molecule. Assuming that paraben aromatic groups occupy ~15 Å^2 in the plane of the lipid monolayer, the area changes would correspond to the presence of 0.1, 0.5, and 1 molecule of ethyl, propyl, and butyl paraben per lipid, respectively. Conversely, at an area per molecule of 68.5 Å^2 (which corresponds to 35 mN/m with no paraben), we observed 5, 12.5, and 20% increases in surface pressure at 1 mM ethyl, propyl, and butyl paraben, respectively. This means that at lipid packing densities characteristic of unstretched membranes, parabens can intercalate and stably reside in the lipid environment, thus perturbing the lateral pressure profile in the membranes. Both the surface activity and magnitude of monolayer swelling at monolayer−bilayer equivalence pressure are commensurate with the hydrophobicity of the molecule.

Effects of Parabens on MscS Activation. MscS channels residing in the inner membrane of *E. coli* are directly sensitive to tension in the lipid bilayer. Suction in the patch pipet creates a pressure gradient across the patch (approximated as a spherical cap) and generates tension according to Laplace (*50*−*52*). In the lipid-reconstituted system, MscS was shown to half-activate at membrane tensions of ~5.5 dyn/cm (*52*). Stimulating the excised patches with ramps of pressure invokes steeply increasing population currents, and saturating ramps or pulses of pressure keep the entire population open. When activated with subsaturating steps of pressure, the channel population shows adaptive responses; i.e., after the initial spike of current passing through a maximum, the channel activity decays with time (*46*). It has been shown previously that the adaptive current decay is due to sequential progression of the channel first into the desensitized (mode-shifted) state and then to the completely inactivated state. Desensitization is a reversible closure from which channels can be reactivated by being stimulated with higher pipet pressures (*53*). If subsaturating tension persists, then channels enter the stretch-insensitive nonconductive inactivated state.

Introduction of parabens into the pipet produced left shifts of activation curves, with the strongest effect observed with the butyl ester. Figure 3A shows such curves for 0.5 mM butyl paraben in response to the 1 s linear ramps of pressure

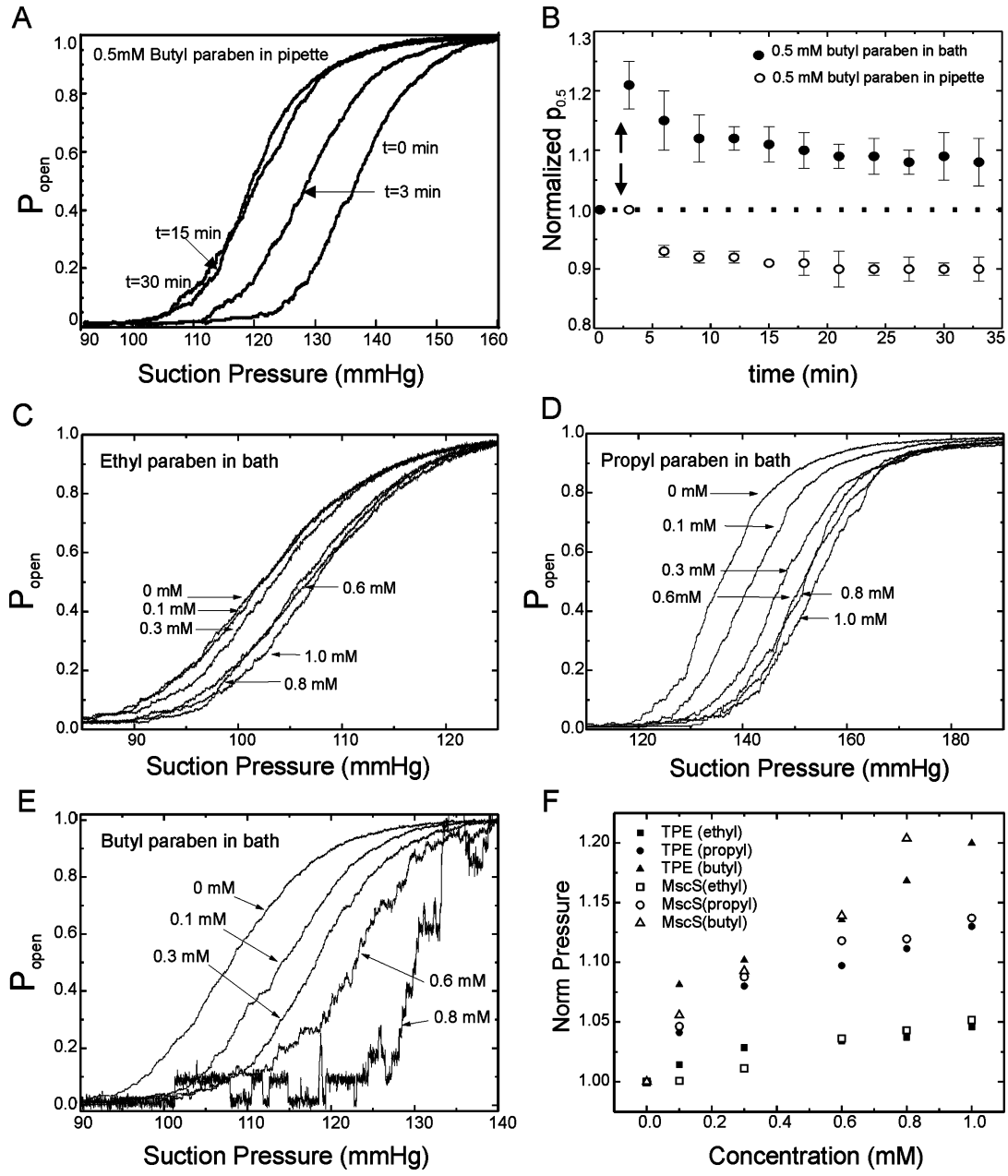

FIGURE 3: Sidedness and concentration dependencies of paraben effects on MscS activation curves measured by linear ramps of pressure. (A) Butyl paraben added through the pipet (0.5 mM) gradually shifts activation points to the left. (B) The kinetics of the activation midpoint ($p_{0.5}$) changes with butyl paraben in the pipet (○) and in the bath (●); the arrows denote either the time of bath perfusion or the moment of seal formation in experiments with paraben in the pipet. MscS activation curves for different concentrations of ethyl (C), propyl (D), and butyl (E) parabens in the bath. Each series was measured on a single patch. (F) Correlation of surface pressure changes measured in monolayers (Figure 2) with the right shifts in the midpoints of activation curves recorded in patch-clamp presented in panels C−E. The surface pressure changes are presented as relative increases at the lipid packing density corresponding to 35 mN/m without paraben. Activation midpoints are also normalized to the midpoint of control curves with no paraben. Both values are presented as functions of paraben concentration.

immediately after ($t = 0$) and 3, 15, and 30 min following formation of a seal. In this experiment, the tip of the pipet was filled with a paraben-free buffer and then back-filled with a paraben-containing buffer. The kinetics of the midpoint shift [Figure 3B (○)] presented in normalized scale likely reflects the diffusion of butyl paraben into the tip and incorporation into the outer leaflet. The midpoint ($p_{0.5}$) decreases monotonously and saturates within 15 min at ~90% of the initial midpoint pressure measured upon patch excision. No decline in the number of active channels was observed. Without employing a pipet-perfusion device, were unable to take measurements at different concentrations of parabens on one patch; thus, we present the time progression of the effect under diffusion-limited delivery of the paraben to the patch.

When ethyl, propyl, or butyl parabens were presented to the cytoplasmic side of excised patches (bath), the MscS activation curves shifted right toward higher opening pressures (Figure 3B−F). It was noticed that the $p_{0.5}$ shifts have a transient component. The kinetics of $p_{0.5}$ changes evoked by perfusion of 0.5 mM butyl paraben into the bath averaged over four independent patches is shown in Figure 3B (●). Approximately 1 min after perfusion (denoted with an arrow), $p_{0.5}$ experiences an ~25% right shift and then gradually

declines to a steady level 8−12% above $p_{0.5}$ measured prior to paraben addition. To record concentration dependencies of $p_{0.5}$ on one patch, measurements were taken 2−3 min after each sequential perfusion of the buffer with a progressively increasing concentration of the paraben. As illustrated in Figure 3C−E, at a concentration of 1 mM in the bath, ethyl paraben, the most hydrophilic of the parabens, shifted the midpoint of activation by 5%, propyl paraben shifted it by 12.5%, and the most hydrophobic among them shifted the midpoint of activation by 25%. Note that butyl paraben, which causes the most drastic shifts, also leads to inactivation of a large population of MscS such that only a small fraction of channels remained active at the end of the 1 s saturating ramp. To compare the midpoint shifts at different concentrations of butyl paraben, the activation curves presented in Figure 3E were normalized to the maximal current achieved at the end of the ramp. Upon washout, the midpoint of activation typically shifted back to the left, and the final curve coincided with the initial control. This indicates that the effect of parabens is reversible and driven by the concentration of the species in the aqueous environment near the lipid membrane. It was observed that 10−20% of the initial channels are not available on washout. In contrast to the previous report (*54*), we did not observe spontaneous activation of MscS by any of the parabens added from either side at a pipet potential of 20 mV.

We presume that the midpoint shifts in opposite directions can be attributed to an asymmetric partitioning of paraben into one of the leaflets thus exerting additional lateral pressure in that particular leaflet and creating tension in the opposite leaflet (*23*−*25, 55*). Indeed, with externally added tension to the entire bilayer, the partitioning of paraben into the cytoplasmic leaflet will exert pressure (or reduce tension) acting on the gate, which should be observed as a right shift of the activation midpoint. The normalized data for MscS activation in patch−clamp and lateral pressure shifts in monolayer experiments are combined in Figure 3F, showing that the magnitudes of activation midpoint shifts for the channel in the presence of each of the three parabens are in good agreement with the data for the concentration-dependent increase in surface pressure in the lipid monolayer at membrane packing densities.

Effects of Parabens on the Kinetics of MscS Adaptation and Recovery. To clarify the nature of the observed decrease in active channels in the presence of high concentrations of parabens (Figure 3E), we looked at the propensity of MscS for the desensitized and inactivated states under similar conditions. In a typical patch−clamp experiment, MscS desensitization is manifested as a gradual current decline over the course of 1−30 s (*45, 46, 56*). If tension persists, then desensitized (mode-shifted and closed) channels make a transition to the nonconducting and stretch insensitive inactivated state (*53*). The entire process of adaptation was shown to be tension-dependent; thus, we tested MscS population responses to a series of subsaturating steps of pressure (Figure 4C), in the presence of various concentrations of paraben. Figure 4A shows control traces that illustrate the initial peak of activity and adaptive current decline at different pressures. The pressure amplitudes spaced by 10 mmHg were chosen around the midpoint of activation which was 140 mmHg for this particular patch as determined with a 1 s saturating ramp prior to stepping. Both the peak of the response and the characteristic decay time depend on stimulus amplitude. As illustrated in Figure 4B, perfusion of 0.8 mM butyl paraben into the bath did not change the peak amplitude of the transient response considerably, but it strongly reduced the current decay time over the entire range of pressures. Both ethyl and propyl paraben show similar but weaker effects on MscS desensitization. These data indicate that parabens do not block channel conduction, as could be inferred from Figure 3E, but rather cause fast desensitization and possibly inactivation. Because the initial peaks of activity in the beginning of pressure steps are comparable (Figure 4A,B), butyl paraben does not drive MscS into the inactivated state from the resting state at subthreshold tensions but strongly accelerates desensitization once the channels are open.

Several stable patches permitted us to collect the decay data for the entire pressure range at six different concentrations for each of the parabens. The results of monoexponential fitting of such data sets for ethyl, propyl, and butyl parabens are shown in Figure 4D. Each panel represents fitting results of a series of 30 traces taken at different concentrations and pressures on a single patch. The pressure on the graph is normalized to the midpoint ($p_{0.5}$) measured in the absence of paraben. Near the midpoint, butyl paraben reduces the characteristic time of decay (τ) by 2 orders of magnitude in the presence of 1 mM paraben, but the extent of τ decrease is uneven across the pressure range; on the left end ($p = 0.8p_{0.5}$), the points collected between 0.6 and 1 mM paraben group tightly, showing that the effect of the amphipath already saturates at these concentrations and the entire rate change is only ~1 order of magnitude. At the right end ($p = 1.14p_{0.5}$), however, all points are well spread out and the entire effect of paraben induces a change in τ of almost 2.5 orders of magnitude. It is obvious that the effect of paraben on the desensitization kinetics increases with tension. Both propyl and ethyl paraben show qualitatively similar although progressively weaker effects on MscS adaptation. The magnitudes of τ change are 0.5 and 0.25 log unit at the left end and 1.3 and 0.8 log units at the right end for propyl and ethyl paraben, respectively. The data strongly suggests that increased membrane tension (proportional to the pipet pressure) favors incorporation of paraben into the membrane which results in larger changes in the rate of adaptation.

In the following experiments, we attempted to separate the two sequential processes, desensitization (O → D) and inactivation (D → I) (*53*). To reveal the desensitized population of channels that can be reactivated from those that are inactivated, the stimulus to a subsaturating pressure was interspersed with short test pulses of saturating pressure. A control trace and a current response to the same stimulus protocol in the presence of ethyl paraben are shown in Figure 5A. The initial decay rate is primarily due to reversible desensitization as most of the channels respond to the first test pulse. The decreasing current responses to subsequent test pulses indicate that the fraction of tension-sensitive channels decreases and the tension-insensitive fraction grows over time. Addition of 0.5 mM ethyl paraben accelerates desensitization, but as revealed by test pulses, the rate of inactivation does not change substantially. Figure 5D shows the pair of traces from a different patch recorded with the same pressure protocol without and with 0.2 mM butyl

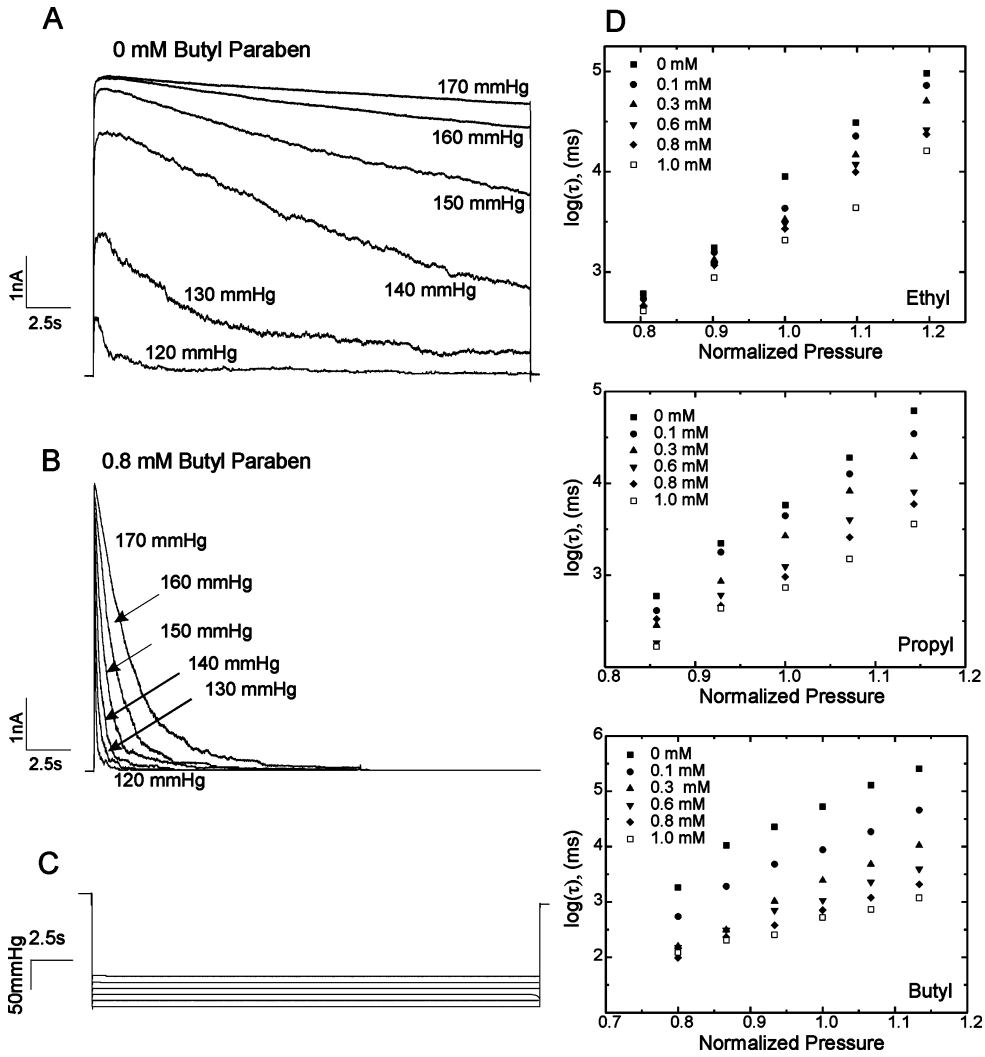

FIGURE 4: Parabens increase the rate of MscS adaptation. (A) Current responses of MscS populations to varied subsaturating steps of pressure without paraben. (B) Adaptive current responses with 0.8 mM butyl paraben on the cytoplasmic (bath) side recorded in the same patch. The step pressure protocol (C) was the same in both experiments. (D) Characteristic time of current decay at different concentrations of ethyl, propyl, and butyl paraben presented as log(τ) vs normalized pressure. The pressure was normalized to $p_{0.5}$ determined in ramp experiments for each patch.

paraben in the bath. In this instance, we observe a marked shortening of the decay time and shortening of the inactivation time as well.

To quantify the rates of desensitization and inactivation, we tabulated several points along these traces. One group of points represented the decaying fraction of conductive channels under subsaturating pressure (i.e., fraction of open channels that is additive to the combined D+I population). Another data group consists of the peaks in response to saturating test pulses that represent the combined population in D+O states. We then fitted the curves with the three-state kinetic model (O → D → I) described by a known set of differential equations (*57*) (see the legend of Figure 5). The graphs in panels B and C of Figure 5 show the fits of the model to the experimental points and the extracted rate constants k_{OD} and k_{DI} for the O → D and D → I steps, respectively. In the presence of ethyl paraben, the rate constant for desensitization (at a given tension) increases, whereas the rate of inactivation actually decreases. Both tendencies are consistent with the qualitative observation that increased membrane tension slows the process of desensitization but accelerates inactivation (Belyy, Akitake, Kamaraju, Anishkin, and Sukharev, manuscript in preparation). Indeed, when ethyl paraben present on the cytoplasmic side intercalates into the membrane creating its own lateral pressure, it negates a large portion of tension in the inner leaflet. As seen from Figure 5D, butyl paraben (0.2 mM) further increases the rate of desensitization, but surprisingly, it also accelerates the rate of inactivation. The increased rate of inactivation was noticed in several patches at higher concentrations of butyl paraben [0.33 and 0.5 mM (data not shown)].

Following complete inactivation, MscS recovers from the inactivated state back to the resting state. The recovery rate appears to be fastest under zero tension. A control trace and a trace recorded in the presence of 0.5 mM ethyl paraben are shown in Figure 6A along with the pulse protocol used to measure the recovery time. Following a subsaturating step of pressure during which the channels are desensitized and inactivated, the available (non-inactivated) fraction is revealed by a short test pulse. The patch pressure is then dropped to zero, and a train of short saturating test pulses is applied to follow the process of recovery. Addition of ethyl paraben shortens the current decay time and leads to a deeper

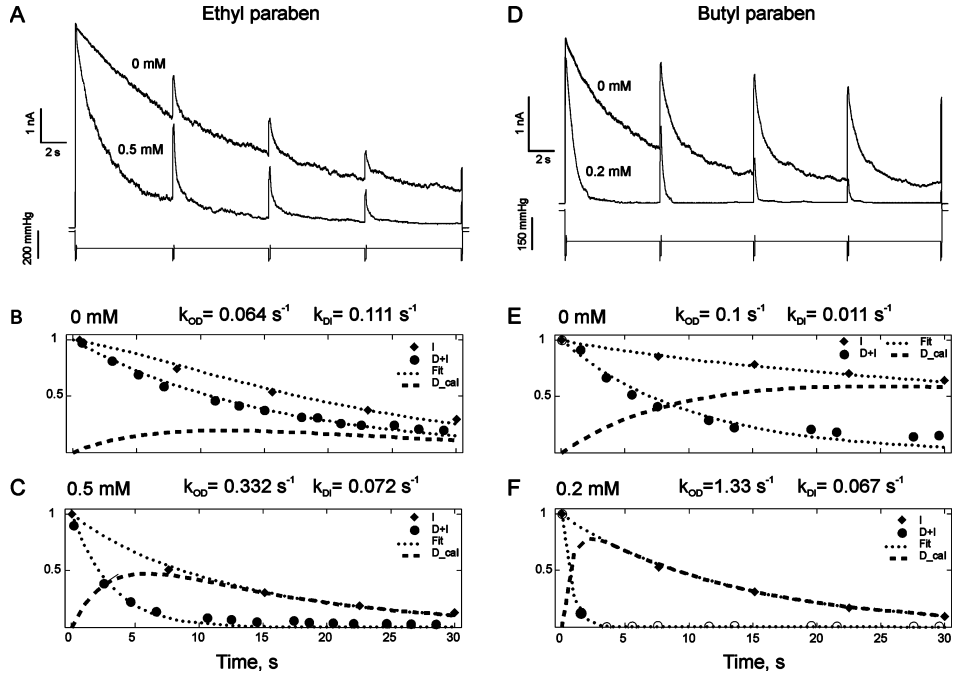

FIGURE 5: Experiment separating MscS desensitization from inactivation. (A) Traces illustrating desensitization and inactivation of MscS with and without 0.5 mM ethyl paraben and the corresponding pressure protocol with interspersed test pulses. Panels B and C show data points representing the combined inactivated and desensitized (D+I) and only inactivated (I) populations with the theoretical fits to determine k_{OD} and k_{DI}. Panels B and C depict results from experiments without and with 0.5 mM ethyl paraben, respectively. (D−F) Experiment analogous that presented in panel A performed with and without 0.2 mM butyl paraben. Fitting of the data was done using analytical solutions of the standard set of differential equations (*57*) describing a three-state kinetic model (O → D → I): $O(t) = O_0\, e^{-k_{OD}t}$; $D(t) = (k_{OD}/k_{DI} - k_{OD})O_0(e^{-k_{OD}t} - e^{-k_{DI}t})$; $I(t) = O_0 - D(t) - I(t)$. In panels B, C, E, and F, the I state (◆) is presented in an inverted scale as in experimental traces (A and D). Circles represent the open population [$O = 1 - (D + I)$]. The intermediate desensitized population (D) was computed (thick dashed line).

inactivation, but the comparison of the time courses for recovery (inset) indicates no change compared to the control. The pair of recovery curves obtained without and with 0.33 mM butyl paraben (Figure 6C) shows that this substance slightly slows the process of recovery, but to a much lesser extent than it shortens the adaptive current decay. So far, parabens exert much weaker effects on the process of MscS recovery than on desensitization or inactivation.

DISCUSSION

The data presented above show that the effects of the three parabens on the mechanosensitive channel MscS strongly correlate with their surface activity at the air−water interface and their potency to modify surface (lateral) pressure of lipid monolayers. The presented monolayer data indicate that at the monolayer−bilayer equivalence pressure butyl paraben packs favorably between phospholipids at a molar ratio near 1:1. The magnitudes of all observed effects, including effects on MscS activation midpoint and adaptation rate, positively correlate with the hydrophobicity of paraben, i.e., the length of its alkyl chain. The results are consistent with the paradigm that the antibacterial action of these substances begins with their partitioning into the membrane. With this regard, can MscS be the primary target for parabens? This is unlikely because MscS is not an essential component of the bacterial cytoplasmic membrane under typical laboratory conditions, and only the double-knockout *mscL*$^-$/*mscS*$^-$ shows compromised viability under severe osmotic shock (*45*). If parabens were strong MscS activators, then "chemical" opening of the channel would dissipate essential gradients in the cell, and this way, parabens would suppress bacterial growth. In the previous study, Nguyen and co-authors (*54*) reported spontaneous activation of MscL in reconstituted liposomes in the presence of 1 mM propyl paraben applied through the pipet, as well as spontaneous activities of MscS-like channels in spheroplast patches exposed to methyl, ethyl, and propyl parabens from the cytoplasmic side. In contrast to that report (*54*), we did not observe any direct activation of MscS by parabens from the cytoplasmic side even with the more hydrophobic and potent butyl ester, and the activation midpoint in our hands shifted to higher values. There was indeed a decrease in the activation midpoint of MscS with butyl paraben added from the pipet side (Figure 3A,B), but never to the point of spontaneous activity at zero pressure. MscS and MscL may not be the main targets for this class of substances because the triple mutant MJF465 (*mscS*$^-$/*mscK*$^-$/*mscL*$^-$) appears to have a sensitivity to parabens similar to that of the wild type. Nevertheless, MscS is sensitive to membrane tension and lateral pressure, and its activity provides a measurable readout of this parameter. Therefore, this channel can be used as a reasonably well-characterized sensor of lateral pressure and tension in the surrounding lipid bilayer (*52, 58*), which is commonplace for all integral proteins in the cell.

The pressure−area diagrams obtained for lipid bilayers indicate that parabens can be stably coordinated between lipids, more favorably at intermediate densities and pressures. While higher lateral pressures make their residence less favorable, still at the monolayer−bilayer equivalence pressures (35−40 mN/m) butyl paraben present at 1 mM is capable of bringing about a 20% increase in the respective pressure. This translates into 7−8 mN/m of lateral pressure

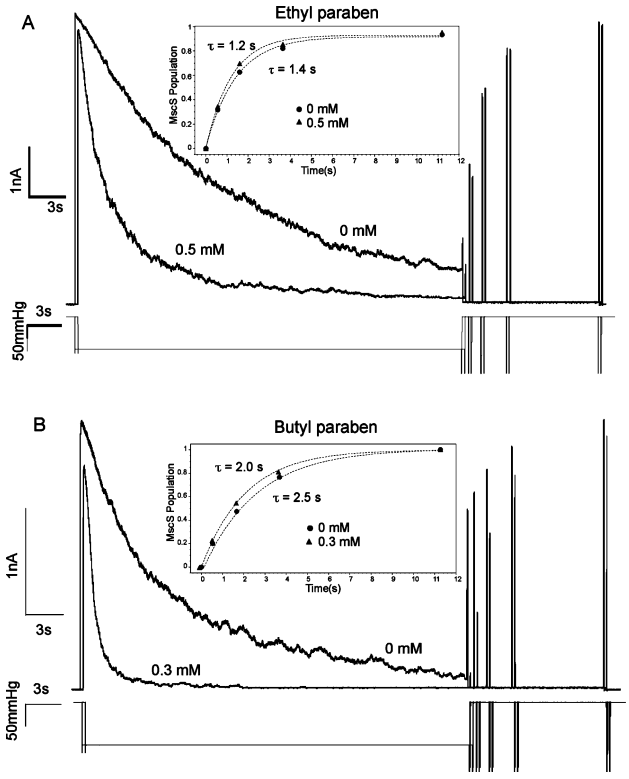

FIGURE 6: Recovery from inactivation of MscS after a prolonged subsaturating step revealed by a train of short test pulses is unaffected by parabens. (A) Traces obtained with 0 and 0.5 mM ethyl paraben on the same patch stimulated with the same pressure protocol shown below. (B) Similar traces recorded with 0 and 0.2 mM butyl paraben in the bath. Insets in each panel represent the time courses for recovery fitted with monoexponential functions.

(tension) change which encompasses almost the entire range of tensions activating MscS [activation midpoint $\gamma = 5.5$ dyn/cm (*52*)]. The monolayer data suggest that when a patch membrane is stretched in the presence of paraben, the amphipathic molecules insert themselves and diminish the tension in the leaflet exposed to paraben. The amount of right shift in activation curves scales well with the pressures detected in monolayers (Figure 3F). Even at high tension in the presence of parabens, the channel quickly adapts but often does not close completely because tension remains in the opposite leaflet.

The direction of the initial shift of activating pressure depends on the side of paraben application. One should remember that the two leaflets of the bilayer are coupled by the midplane area. Intercalation of an amphipath in one leaflet expands its area and at the same time creates tension in the opposite leaflet (*23*−*25*), whereas the total tension in the bilayer may remain constant. Paraben applied externally is expected to generate tension in the inner leaflet, thus shifting activating pressure to the left. When added from the cytoplasmic side, parabens shift MscS activating pressure to the right, but after reaching the maximum, the effect declines to a lower level. Indeed, initial incorporation of the substance into the inner leaflet would produce the maximal asymmetry of pressure−tension distribution, but subsequent permeation into the periplasmic leaflet would decrease this asymmetry. The steady-state shift observed in the system suggests that with a concentration gradient, paraben may never be equalized completely in the two leaflets as it can partition into the aqueous solution on the other side. In the absence of buffer convection in the narrow tip of the pipet, however, paraben accumulation in the periplasmic leaflet can be substantial. In the reverse configuration when paraben is added through the pipet, the decrease in $p_{0.5}$ is steady possibly because paraben traversing the bilayer does not accumulate in the inner leaflet as it washes away into the large paraben-free bath compartment.

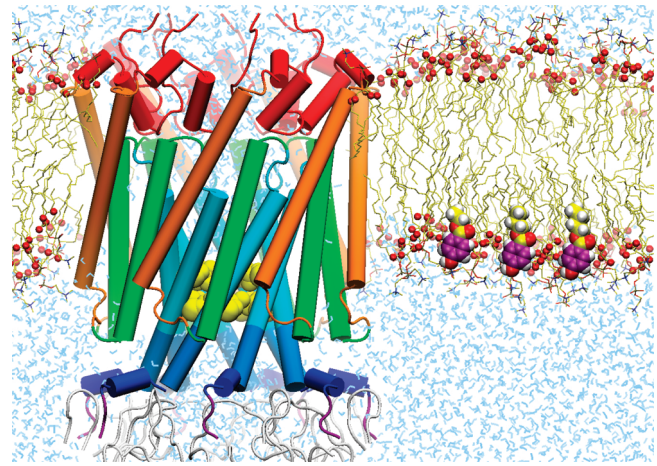

FIGURE 7: Model of resting MscS in the lipid bilayer and the predicted positions of the gate and the three parabens bound to the inner leaflet. The model was derived from the original crystal structure (PDB entry 1MXM) by aligning the peripheral helices TM1 (orange) and TM2 (green) with the pore-lining TM3 helices (blue). The structure of the N-terminal domain (red) was predicted and added to the structure, and the model of the resting state of MscS was equilibrated in the POPC bilayer for 12 ns (taken from ref *59*). The gate leucines (L105 and L109) inside the TM3 barrel are shown as yellow VdW spheres, and their position is ∼7 Å below the layer of carbonyl and glycerol oxygens of phospholipids (red dots) approximating the membrane interface. Incorporation of parabens into the inner leaflet of the lipid bilayer is expected near this apolar−polar interface. The created peak of lateral pressure not far from the gate is predicted to collapse the barrel into a nonconductive state.

Why do cytoplasmic additions of parabens increasing pressure in the inner leaflet shift the activation midpoint specifically to the right? Figure 7 depicts the resting model of the transmembrane domain of MscS (*59*) derived from its crystal structure (*60*). In the simulation described by Anishkin and co-workers (*59*), this model was thoroughly equilibrated in the lipid bilayer. The position of the channel gate (yellow surface) inside the central barrel is decisively cytoplasmic; thus, increased pressure in the inner leaflet is expected to "squeeze" gate. The observed shifts in the dose−response curves reflect this picture and are consistent with previous observations with TFE (*61*). Providing this qualitative explanation to the observed shifts, we should mention that at present the exact position of the absorbed paraben in the bilayer is unknown. It is likely that the benzyl ring will pack next to glycerol and carbonyl groups as predicted by the most favorable location of aromatic side chains in membrane proteins (*62*). The layer of oxygens belonging to these groups (depicted as red dots in Figure 7) is located not far (∼7 Å) from the gate, and therefore, incorporation of parabens near the apolar−polar interface would create a peak of lateral pressure that would tend to collapse the channel barrel to its nonconductive state.

The observed difference between effects of ethyl and butyl parabens on inactivation is puzzling. Indeed, ethyl paraben

acted as a tension-reducing agent and decreased the rate of inactivation following desensitization. Butyl paraben, in contrast, dramatically increased the rate of inactivation. One possible difference could be that more potent butyl paraben creates a stronger lateral pressure peak that not only collapses the gate but also leads to fast propagation of the TM3 kink up the helix from G121 to G113. Buckling of the TM3 helix at G121 was ascribed to closing and desensitization, whereas bending at G113 was associated specifically with channel inactivation (*53*). The difference could also be due to the higher hydrophobicity of butyl paraben and therefore different preferred position in the membrane compared to less hydrophobic ethyl paraben, creating a peak of pressure at a different location. Both hypotheses warrant further experiments describing tension and concentration dependencies of different parabens on these processes. The experimental observations also call for detailed molecular dynamics simulations that would suggest the preferred positions of these substances in the lipid bilayer and the magnitudes of local pressure changes induced by their incorporation.

Generally, the observed effects of parabens on the kinetics of adaptation resemble effects of trifluoroethanol (TFE) with one difference being that TFE did slow the rate of recovery from the inactivated state (*61*). This was explained as intercalation of small TFE molecules into the TM2−TM3 crevices which were predicted to disrupt the tension transmission route from the periphery to the gate. Penetration of TFE would stabilize these crevices and prevent fast recovery. Because parabens did not exhibit any systematic effect on recovery, we conclude that they do not penetrate and stabilize the crevices.

ACKNOWLEDGMENT

We thank Dr. Andriy Anishkin for critical discussion and for providing the MscS simulation snapshot (Figure 7). We also thank Mrs. Naili Liu for technical assistance with spheroplasts.

REFERENCES

1. Cornell, R. B., and Taneva, S. G. (2006) Amphipathic helices as mediators of the membrane interaction of amphitropic proteins, and as modulators of bilayer physical properties. *Curr. Protein Pept. Sci. 7*, 539–552.
2. Rebecchi, M., Bonhomme, M., and Scarlata, S. (1999) Role of lipid packing in the activity of phospholipase C-δ1 as determined by hydrostatic pressure measurements. *Biochem. J. 341* (Part 3), 571–576.
3. Botelho, A. V., Huber, T., Sakmar, T. P., and Brown, M. F. (2006) Curvature and hydrophobic forces drive oligomerization and modulate activity of rhodopsin in membranes. *Biophys. J. 91*, 4464–4477.
4. Tillman, T. S., and Cascio, M. (2003) Effects of membrane lipids on ion channel structure and function. *Cell Biochem. Biophys. 38*, 161–190.
5. Ding, X. Q., Fitzgerald, J. B., Matveev, A. V., McClellan, M. E., and Elliott, M. H. (2008) Functional activity of photoreceptor cyclic nucleotide-gated channels is dependent on the integrity of cholesterol- and sphingolipid-enriched membrane domains. *Biochemistry 47*, 3677–3687.
6. Schmidt, D., Jiang, Q. X., and MacKinnon, R. (2006) Phospholipids and the origin of cationic gating charges in voltage sensors. *Nature 444*, 775–779.
7. Xu, Y., Ramu, Y., and Lu, Z. (2008) Removal of phospho-head groups of membrane lipids immobilizes voltage sensors of K^+ channels. *Nature 451*, 826–829.
8. Hilgemann, D. W., Feng, S., and Nasuhoglu, C. (2001) The complex and intriguing lives of PIP2 with ion channels and transporters. *Sci STKE. 2001*, RE19.
9. Curnow, P., Lorch, M., Charalambous, K., and Booth, P. J. (2004) The reconstitution and activity of the small multidrug transporter EmrE is modulated by non-bilayer lipid composition. *J. Mol. Biol. 343*, 213–222.
10. Michalak, K., Wesolowska, O., Motohashi, N., Molnar, J., and Hendrich, A. B. (2006) Interactions of phenothiazines with lipid bilayer and their role in multidrug resistance reversal. *Curr. Drug Targets 7*, 1095–1105.
11. Marsh, D. (1996) Lateral pressure in membranes. *Biochim. Biophys. Acta 1286*, 183–223.
12. Cantor, R. S. (1998) The lateral pressure profile in membranes: A physical mechanism of general anesthesia. *Toxicol. Lett. 100−101*, 451–458.
13. Lindahl, E., and Edholm, O. (2000) Spatial and energetic-entropic decomposition of surface tension in lipid bilayers from molecular dynamics simulations. *J. Chem. Phys. 113*, 3882–3893.
14. Marsh, D. (2007) Lateral pressure profile, spontaneous curvature frustration, and the incorporation and conformation of proteins in membranes. *Biophys. J. 93*, 3884–3899.
15. Gullingsrud, J., and Schulten, K. (2004) Lipid bilayer pressure profiles and mechanosensitive channel gating. *Biophys. J. 86*, 3496–3509.
16. Connelly, T. J., and Coronado, R. (1994) Activation of the Ca^{2+} release channel of cardiac sarcoplasmic reticulum by volatile anesthetics. *Anesthesiology 81*, 459–469.
17. Zimmerman, S. A., Jones, M. V., and Harrison, N. L. (1994) Potentiation of γ-aminobutyric acidA receptor Cl^- current correlates with in vivo anesthetic potency. *J. Pharmacol. Exp. Ther. 270*, 987–991.
18. Franks, N. P., and Lieb, W. R. (1997) Inhibitory synapses. Anaesthetics set their sites on ion channels. *Nature 389*, 334–335.
19. Krasowski, M. D., and Harrison, N. L. (1999) General anaesthetic actions on ligand-gated ion channels. *Cell. Mol. Life Sci. 55*, 1278–1303.
20. Cantor, R. S. (2001) Breaking the Meyer-Overton rule: Predicted effects of varying stiffness and interfacial activity on the intrinsic potency of anesthetics. *Biophys. J. 80*, 2284–2297.
21. Seelig, A., Allegrini, P. R., and Seelig, J. (1988) Partitioning of local anesthetics into membranes: Surface charge effects monitored by the phospholipid head-group. *Biochim. Biophys. Acta 939*, 267–276.
22. Fischer, H., Gottschlich, R., and Seelig, A. (1998) Blood-brain barrier permeation: Molecular parameters governing passive diffusion. *J. Membr. Biol. 165*, 201–211.
23. Heerklotz, H. (2001) Membrane stress and permeabilization induced by asymmetric incorporation of compounds. *Biophys. J. 81*, 184–195.
24. Traikia, M., Warschawski, D. E., Lambert, O., Rigaud, J. L., and Devaux, P. F. (2002) Asymmetrical membranes and surface tension. *Biophys. J. 83*, 1443–1454.
25. Markin, V. S., and Martinac, B. (1991) Mechanosensitive ion channels as reporters of bilayer expansion. A theoretical model. *Biophys. J. 60*, 1120–1127.
26. Perozo, E., Kloda, A., Cortes, D. M., and Martinac, B. (2002) Physical principles underlying the transduction of bilayer deformation forces during mechanosensitive channel gating. *Nat. Struct. Biol. 9*, 696–703.
27. Moe, P., and Blount, P. (2005) Assessment of potential stimuli for mechano-dependent gating of MscL: Effects of pressure, tension, and lipid headgroups. *Biochemistry 44*, 12239–12244.
28. Chemin, J., Patel, A., Duprat, F., Zanzouri, M., Lazdunski, M., and Honore, E. (2005) Lysophosphatidic acid-operated K^+ channels. *J. Biol. Chem. 280*, 4415–4421.
29. Honore, E. (2007) The neuronal background K2P channels: Focus on TREK1. *Nat. Rev. Neurosci. 8*, 251–261.
30. Soni, M. G., Burdock, G. A., Taylor, S. L., and Greenberg, N. A. (2001) Safety assessment of propyl paraben: A review of the published literature. *Food Chem. Toxicol. 39*, 513–532.
31. Alexander, K. S., Laprade, B., Mauger, J. W., and Paruta, A. N. (1978) Thermodynamics of aqueous solutions of parabens. *J. Pharm. Sci. 67*, 624–627.
32. Giordano, F., Bettini, R., Donini, C., Gazzaniga, A., Caira, M. R., Zhang, G. G., and Grant, D. J. (1999) Physical properties of parabens and their mixtures: Solubility in water, thermal behavior, and crystal structures. *J. Pharm. Sci. 88*, 1210–1216.

33. Perlovich, G. L., Rodionov, S. V., and Bauer-Brandl, A. (2005) Thermodynamics of solubility, sublimation and solvation processes of parabens. *Eur. J. Pharm. Sci. 24*, 25–33.
34. Fukahori, M., Akatsu, S., Sato, H., and Yotsuyanagi, T. (1996) Relationship between uptake of p-hydroxybenzoic acid esters by *Escherichia coli* and antibacterial activity. *Chem. Pharm. Bull. 44*, 1567–1570.
35. Kleinfeld, J., and Ellis, P. P. (1967) Inhibition of Microorganisms by Topical Anesthetics. *Appl. Microbiol. 15*, 1296–1298.
36. Ma, Y., and Marquis, R. E. (1996) Irreversible paraben inhibition of glycolysis by Streptococcus mutans GS-5. *Lett. Appl. Microbiol. 23*, 329–333.
37. Doron, S., Friedman, M., Falach, M., Sadovnic, E., and Zvia, H. (2001) Antibacterial effect of parabens against planktonic and Biofilm *Streptococcus sobrinus*. *Int. J. Antimicrob. Agents 18*, 575–578.
38. Golden, R., Gandy, J., and Vollmer, G. (2005) A review of the endocrine activity of parabens and implications for potential risks to human health. *Crit. Rev. Toxicol. 35*, 435–458.
39. Bairati, C., Goi, G., Lombardo, A., and Tettamanti, G. (1994) The esters of p-hydroxy-benzoate (parabens) inhibit the release of lysosomal enzymes by mitogen-stimulated peripheral human lymphocytes in culture. *Clin. Chim. Acta 224*, 147–157.
40. Nakagawa, Y., and Moore, G. (1999) Role of mitochondrial membrane permeability transition in p-hydroxybenzoate ester-induced cytotoxicity in rat hepatocytes. *Biochem. Pharmacol. 58*, 811–816.
41. Inoue, K., Nakazawa, K., Inoue, K., Fujimori, K., and Takanaka, A. (1994) Modulation by alkyl p-hydroxybenzoates of voltage- and ligand-gated channels in peripheral neuronal cells. *Neuropharmacology 33*, 891–896.
42. Fujita, F., Moriyama, T., Higashi, T., Shima, A., and Tominaga, M. (2007) Methyl p-hydroxybenzoate causes pain sensation through activation of TRPA1 channels. *Br. J. Pharmacol. 151*, 153–160.
43. Haynes, W. J., Zhou, X. L., Su, Z. W., Loukin, S. H., Saimi, Y., and Kung, C. (2008) Indole and other aromatic compounds activate the yeast TRPY1 channel. *FEBS Lett. 582*, 1514–1518.
44. Martinac, B., Buechner, M., Delcour, A. H., Adler, J., and Kung, C. (1987) Pressure-sensitive ion channel in *Escherichia coli*. *Proc. Natl. Acad. Sci. U.S.A. 84*, 2297–2301.
45. Levina, N., Totemeyer, S., Stokes, N. R., Louis, P., Jones, M. A., and Booth, I. R. (1999) Protection of *Escherichia coli* cells against extreme turgor by activation of MscS and MscL mechanosensitive channels: Identification of genes required for MscS activity. *EMBO J. 18*, 1730–1737.
46. Akitake, B., Anishkin, A., and Sukharev, S. (2005) The "dashpot" mechanism of stretch-dependent gating in MscS. *J. Gen. Physiol. 125*, 143–154.
47. Perlovich, G. L., Volkova, T. V., Manin, A. N., and Bauer-Brandl, A. (2008) Influence of position and size of substituents on the mechanism of partitioning: A thermodynamic study on acetaminophens, hydroxybenzoic acids, and parabens. *AAPS PharmSciTech 9*, 205–216.
48. Clausell, A., Busquets, M. A., Pujol, M., Alsina, A., and Cajal, Y. (2004) Polymyxin B-lipid interactions in Langmuir-Blodgett monolayers of *Escherichia coli* lipids: A thermodynamic and atomic force microscopy study. *Biopolymers 75*, 480–490.
49. Lopez-Montero, I., Arriaga, L. R., Monroy, F., Rivas, G., Tarazona, P., and Velez, M. (2008) High fluidity and soft elasticity of the inner membrane of *Escherichia coli* revealed by the surface rheology of model Langmuir monolayers. *Langmuir 24*, 4065–4076.
50. Opsahl, L. R., and Webb, W. W. (1994) Lipid-glass adhesion in giga-sealed patch-clamped membranes. *Biophys. J. 66*, 75–79.
51. Sukharev, S. I., Sigurdson, W. J., Kung, C., and Sachs, F. (1999) Energetic and spatial parameters for gating of the bacterial large conductance mechanosensitive channel, MscL. *J. Gen. Physiol. 113*, 525–540.
52. Sukharev, S. (2002) Purification of the small mechanosensitive channel of *Escherichia coli* (MscS): The subunit structure, conduction, and gating characteristics in liposomes. *Biophys. J. 83*, 290–298.
53. Akitake, B., Anishkin, A., Liu, N., and Sukharev, S. (2007) Straightening and sequential buckling of the pore-lining helices define the gating cycle of MscS. *Nat. Struct. Mol. Biol. 14*, 1141–1149.
54. Nguyen, T., Clare, B., Guo, W., and Martinac, B. (2005) The effects of parabens on the mechanosensitive channels of *E. coli*. *Eur. Biophys. J. 34*, 389–395.
55. Markin, V. S., and Sachs, F. (2004) Thermodynamics of mechanosensitivity. *Phys. Biol. 1*, 110–124.
56. Koprowski, P., and Kubalski, A. (1998) Voltage-independent adaptation of mechanosensitive channels in *Escherichia coli* protoplasts. *J. Membr. Biol. 164*, 253–262.
57. Houston, P. L. (2001) *Chemical Kinetics and Reaction Dynamics*, Dover, Mineola, NY.
58. Okada, K., Moe, P. C., and Blount, P. (2002) Functional design of bacterial mechanosensitive channels. Comparisons and contrasts illuminated by random mutagenesis. *J. Biol. Chem. 277*, 27682–27688.
59. Anishkin, A., Akitake, B., and Sukharev, S. (2008) Characterization of the resting MscS: Modeling and analysis of the closed bacterial mechanosensitive channel of small conductance. *Biophys. J. 94*, 1252–1266.
60. Bass, R. B., Strop, P., Barclay, M., and Rees, D. C. (2002) Crystal structure of *Escherichia coli* MscS, a voltage-modulated and mechanosensitive channel. *Science 298*, 1582–1587.
61. Akitake, B., Spelbrink, R. E., Anishkin, A., Killian, J. A., de Kruijff, B., and Sukharev, S. (2007) 2,2,2-Trifluoroethanol changes the transition kinetics and subunit interactions in the small bacterial mechanosensitive channel MscS. *Biophys. J. 92*, 2771–2784.
62. White, S. H., and Wimley, W. C. (1999) Membrane protein folding and stability: Physical principles. *Annu. Rev. Biophys. Biomol. Struct. 28*, 319–365.

BI801092G